

Triangulation of Well-Defined Points as a Constraint for Reliable Image Matching

Qing Zhu, Jie Zhao, Hui Lin, and Jianya Gong

Abstract

This study demonstrates the utilization of the well-defined points to improve the reliability and accuracy of image matching. The basic principle is: (a) to triangulate a few well-defined points within the stereo model area to form a coarse triangulation; (b) to detect certain amount of corners within each triangle for further matching; (c) to propagate the matching of corner points from the reference points (i.e., the three triangle vertices) to obtain the best matching for each of these corners; (d) to dynamically update the triangulation by inserting the newly matched corner; and (e) to further detect corners and perform matching for them until a pre-defined criteria (the minimum size of triangle or the largest number of points matched) is reached. Experimental results reveal: (a) the false matching caused by the occlusion and repetitive texture is diminished; (b) the accuracy is improved, i.e., with a reduction of RMSE of check points (located in different types of terrain areas) by 12 percent to 62 percent, and a reduction of the largest error by up to two times; and (c) most building corners and boundary points of main objects could be matched directly and accurately.

Introduction

Digital photogrammetry is a technique used for the derivation of geometric, radiometric, and semantic information of objects in the 3D real world from stereo pairs, i.e., 2D digital images. One of the difficult tasks in digital photogrammetry is image matching, which is a process to automatically search for conjugate points in the overlapping area of a stereo pair, so as to compute object coordinates in a three-dimensional ground coordinate system. Image matching works well in open areas with relatively smooth terrain. However, there are still many problems with larger scale images (i.e., with fine texture), especially in the areas of forest vegetation, settlements, and water bodies (Heipke, 1993; 2001). For example, the problem of completeness is evident in the resulting digital surface models obtained by traditional matching technique, e.g., the corners of buildings and some object boundary points are sometimes not matched. In other words, the reliability of image matching is still difficult in many cases.

Image matching is an ill-posed problem in some circumstances. This is because, for a given point in one image, there might be no conjugate point on the other image of the

stereo pair due to occlusion, or there may be more than one possible candidate as its conjugate point due to repetitive texture (Heipke, 1997). In order to solve such an ill-posed problem, one usually has to find an optimization function to narrow down the searching area. In this way, relatively reliable initial parallax values of the conjugate point to be determined are obtained, so as to minimize potential mismatching.

Ill-posed problems can be converted to well-posed problems by introducing additional knowledge about the problem. The most popular prior knowledge is the epipolar geometry constraint resulting from the calculation of orientation parameters (Heipke, 1996). Although this constraint can reduce the search to one-dimension from two, the match reliability is still not improved distinctly for the above-mentioned cases. Matching reliability can be improved if another two constraints, i.e., the continuity and order, are enforced. In that case, the matching will be done pixel by pixel along each epipolar line, where each pixel's parallax will be dependent on its previous neighbor, reducing the search to a minimum. However, these two constraints are not always satisfied in stereo images. In particular, the order might be violated with transparent (or overlapping) objects, and the continuity does not hold at object boundaries. The order constraint is less important since it does not have a significant effect on the computational efficiency of the whole matching process. On the other hand, the continuity constraint is far more important, and together with the epipolar constraint, is responsible for reducing most of the computational time (Boufama and Jin, 2002). The satisfaction of the continuity/discontinuity constraints was addressed by several researchers recently. In particular, the match propagation method proposed by Lhuillier and Quan (2000) has two most distinctive features, i.e., a match propagation strategy developed by analogy to region growing and a successive regulation by local and global geometric constraints. However, in this method a plane homography of parallax should be tentatively fitted to all the matched points of a grid patch to look for the local potential planar patches. The stability of the homography fitting decreases with the patch size; it is therefore difficult to automatically define a proper cell size of the grid used to subdivide the image into grid patches. Otherwise, Boufama and Jin (2002) developed a hybrid matching algorithm which segments the image into edge and non-edge areas and applies different matching strategies to these two types of areas in order to obtain an optimal results. This matching process is simply

Qing Zhu, Jie Zhao and Jianya Gong are with the State Key Lab of Information Engineering in Surveying Mapping and Remote Sensing (Wuhan University), 29 LuoYu Road, Wuhan, 430079 P.R.China.

Qing Zhu and Hui Lin are with the Joint Laboratory for GeoInformation Science, The Chinese University of Hong Kong, Shatin, New Territories, Hong Kong.

Photogrammetric Engineering & Remote Sensing
Vol. 71, No. 9, September 2005, pp. 1063–1069.

0099-1112/05/7109-1063/\$3.00/0
© 2005 American Society for Photogrammetry
and Remote Sensing

based on the epipolar line constraint and the hypothesis of a smooth surface for non-edge regions; there are still difficulties for the reliable matching of real images with poor texture. A Voronoi diagram-based stereo matching algorithm was proposed by Tang *et al.* (2002). This method attempts to use N seed points (reliably matched feature points) to subdivide the whole image into N Voronoi Cells, and then, the corresponding relations are propagated from the seed in each cell until all pixels within this cell are processed. It is obvious that a number of seed points within symmetrical distribution over the whole image are critical for the good performance of matching result. However, it is still a problem to obtain enough reliable seed points automatically.

This paper proposes a new matching method to control the computational complexity and to ensure high reliability of the results. This method utilizes traditional epipolar geometry and local continuity constraints based on adaptive triangulation of well-defined points. Here, well-defined points stand for symmetrically-distributed and correctly-matched prominent image corner points. Each triangle forms a local continuity constraint area for matching, in which the match will be propagated. Adaptive triangulation means that the triangulation will be dynamically refined by inserting a new matched point. The match propagation refers to the use of prior information relating to previously matched points to generate new matching points. Based on the adaptive triangulation constraint, this method improves the performance of automatic image matching.

This paper is divided into six sections: following this introduction, the second section outlines the principle of the new image matching strategy. The details are then described followed by experimental results with real image pairs, which demonstrate the accuracy and the reliability of the method. Finally, some concluding remarks are given.

The Principle of Triangulation Constraint by Means of Well-defined Points for Image Matching

During the relative orientation and automatic aerial triangulation (as a dense tie points pattern) process, the number of matching candidate points, which are selected automatically or semi-automatically for each image, could exceed several hundred. After a sophisticated gross error detection and removal, the remaining (points primarily situated in good texture positions and successfully matched) can be considered as the initial well-defined points, and thus utilized as reliable prior knowledge for posterior dense image matching. Since the terrain surface is considered as either continuous smooth surface or discontinuous broken surface, it is noticeable that most of the well-defined points are located on the edge of break areas. From this point of view, the authors propose that the coarser characteristics of terrain patches, which are triangles formed by the nearest well-defined points, are regarded as planar surfaces in the object space. This kind of continuity constraint is also correct for parallax in the image space based on the photographic geometry. Based on the local continuity constraint, the possible corners of the finer relief units in each triangle areas are extracted as match candidates, and then, the coarse triangulation is refined into a finer triangulation by inserting the best-matched corner point in it. The matching propagation process (including the corners extraction, the matching propagation, and the triangulation refining) is implemented iteratively until the density of the final matched points is accepted.

In summary, the basic principle of the new matching method is:

1. To triangulate a few well-defined points within the stereo model area to form two corresponding coarse triangulations;

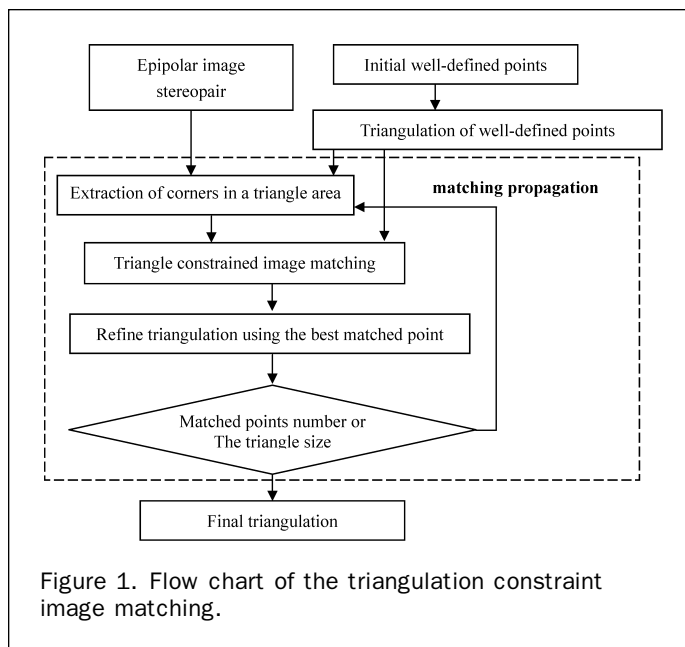


Figure 1. Flow chart of the triangulation constraint image matching.

2. To detect a certain amount of corners within each corresponding triangles Δabc and $\Delta a'b'c'$ for further matching, i.e., detection of corner points $\{p_i; 1 \leq i \leq n\}$ in Δabc and $\{p'_j; 1 \leq j \leq n\}$ in $\Delta a'b'c'$ ($n \approx 5$ to 8);
3. To locate for each corner, e.g., p , its neighboring triangle Δabc and to choose the reference-point amongst a , b , and c : the one with maximal ratio of reliability and its distance to p , i.e., $Max \{\psi(a, a')/Dist(a, p), \psi(b, b')/Dist(b, p), \psi(c, c')/Dist(c, p)\}$. Here, the matching reliability measurement $\psi(a, a')$ is a numerical indicator which measures the quality and reliability of the correlativity between a conjugate point-pair (a, a') as Equation 6;
4. To propagate the matching from the reference points (e.g., a, a') to corner point p , i.e., for each corner p'_j ($1 \leq j \leq n$) in $\Delta a'b'c'$: if it satisfies the condition defined by Equation 4, then compute $\psi(p, p'_j)$. If there are more than one corner of p'_j satisfying the condition defined by Equation 4, only the corner with maximal $\psi(p, p'_j)$ is selected as the best conjugate point p' in $\Delta a'b'c'$ for corner p , and the stereo corners (p, p') are then inserted into the stereo triangulations, respectively; and
5. To further detect corners in new triangles and perform matching propagation until a pre-defined criteria (the minimum size of triangle or the largest matched points number) is reached.

The flow chart of the new matching algorithm is shown in Figure 1, and the key issues of this algorithm are discussed in detail in the coming sections.

Image Matching Algorithm Based on the Triangulation Constraint

Initial Well-defined Points and Their Triangulation

In the general work flow of an existing commercial digital photogrammetric workstation (DPW), a set of conjugate point pairs are generated during relative orientation or automatic aerial triangulation: evenly distributed image corner points are extracted from both images and then matched using the correlation techniques. These corrected, matched points are used to calculate the epipolar geometry, which is then used as a constraint to convert the latter matching procedure from two-dimensional search problem to a one-dimensional search problem. These well-defined points are used to construct the initial coarse triangulation (See Figure 2), in

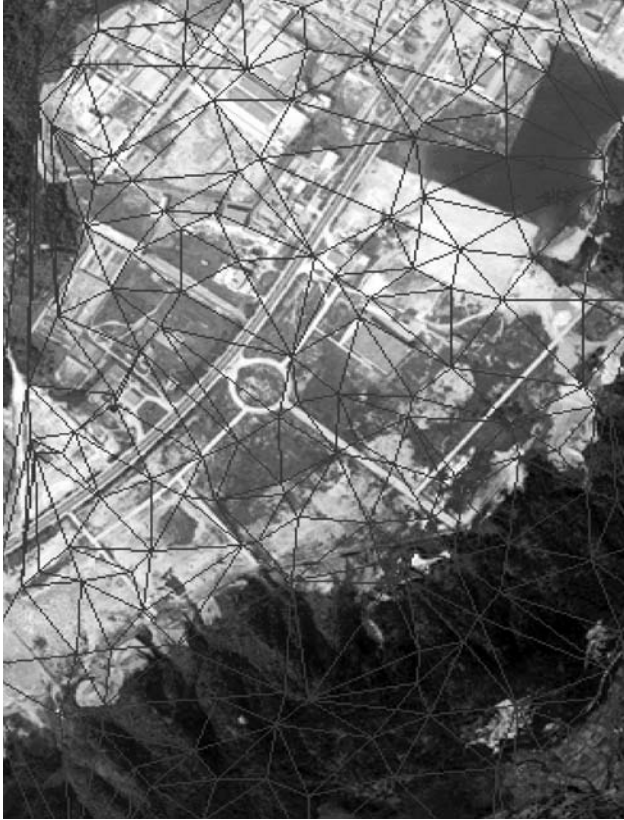


Figure 2. The Delaunay triangulation of the initial well-defined points.

which each triangle forms a local constraint area with three matched points as vertices. In order to triangulate the most nearest points, the Delaunay triangulation is a good choice due to its convenient dynamic generation with unique characteristics and good geometry to random distributed sparse points (Tuceryan and Chorzempa, 1991; Bern and Eppstein, 1992; Li and Zhu, 2003). The Delaunay triangulation of a point set is a collection of edges satisfying an “empty circle” property: for each triangle we can find a circle containing the triangle’s vertices but not containing any other points. Delaunay triangulation is also well-known as the geometric dual of the Voronoi diagram (a collection of geometric objects is a partition of space into cells, each of which consists of the points closer to one particular object than to any others). Because the triangulation will be iteratively refined during the matching propagation procedure, the incremental insertion algorithm of triangulation is adopted (Lawson, 1977).

Matching Propagation

Matching propagation refers to the propagation of matching relations from matched reference points to undetermined corner points. As shown in Figure 1, the triangle continuity constraint is used through the propagation procedure.

The first step of matching propagation is to detect a certain amount of image corner points within a triangle to be processed as the matching candidates from the epipolar stereopair. The choice of corner detector is primarily based on two criteria: repeatability rate and information content. The repeatability rate evaluates the geometric stability under different transformations, which is defined as the

number of points repeated between two images with respect to the total number of detected points. The information content is a measure of the distinctiveness of a detected corner. Schmid *et al.* (2000) evaluated different corner detectors using these two criteria, and concluded that the Harris corner detector satisfies these two criteria best. Therefore, in each triangular constraint area of the stereopair, a set of prominent corners (e.g., five to eight point-pairs in our experiment) are detected out using the Harris corner detector during the propagation procedure. For example, let p_i, p'_j , ($i = 1 \dots n, j = 1 \dots n'$) be the extracted corner points from the two corresponding propagation areas. Let $P = \{p_i; i = 1 \dots n\}$, $P' = \{p'_j; j = 1 \dots n'\}$ be corner sets respectively.

The second propagation step is the triangle constrained matching. Supposing that the potential matching point-pair are (p_i, p'_j) , $p_i \in P, p'_j \in P'$, their parallax should to some degree be related to that of the reference points, such as the point (a, a') shown in Figure 3. Their parallax gradient is defined to be the ratio of their difference in parallax to their distance plus $(\rho_p - \rho_a)/2$ in the image (Zhang and Shan, 2000):

$$PG = \frac{|\rho_p - \rho_a|}{|Dist_{pa} + (\rho_p - \rho_a)/2|} \quad (1)$$

where, $Dist_{pa}$ denotes the Euclidean distance between p_i and a . Experiments in psychophysics have provided evidence that human perception imposes the constraint that the parallax gradient PG is upper-bounded by a limit K , where K is a coefficient relating to psychophysics. The parallax gradient limit K is a free parameter, which can be varied over a range (0, 2). The theoretical limit for an opaque surface is $K = 2$ (Pollard *et al.*, 1986), although the range of allowable surface is extensive with this value, and disambiguating power is weak because false matches receive and exchange as much support as correct ones. “An intermediate value, e.g., between 0.5 and 1 (in our experiment, as a good choice the value 1 was employed), allow selection of a convenient trade-off point between allowable scene surface jaggedness and disambiguating power because it turns out that most false matches produce relatively high parallax gradients” (Zhang and Shan, 2000). That is, if a point on an object is perceived, its neighboring points having $PG > K$ are simply not perceived correctly. Then, imposed by the gradient limit constraint $PG \leq K$, there is in Equation 2 from Equation 1:

$$|\rho_p - \rho_a| \leq K|Dist_{pa} + (\rho_p - \rho_a)/2|. \quad (2)$$

Using inequation $|v_1 + v_2| \leq |v_1| + |v_2|$ for any vectors v_1 and v_2 , there is

$$|\rho_p - \rho_a| \leq KDist_{pa} + K|(\rho_p - \rho_a)/2| \quad (3)$$

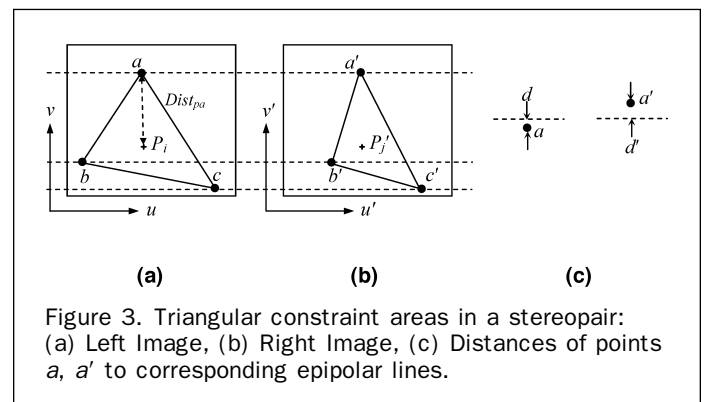


Figure 3. Triangular constraint areas in a stereopair: (a) Left Image, (b) Right Image, (c) Distances of points a, a' to corresponding epipolar lines.

which leads immediately, for $K < 2$, to

$$|\rho_p - \rho_a| \leq \frac{2K}{2-K} \text{Dist}_{pa}. \quad (4)$$

Given a candidate match point p_i in the neighborhood of a , its conjugate point p'_i that satisfies the parallax gradient constraint with limit K must be inside a disk centered at $p_i + \rho_a$ with radius equal to $\frac{2K}{2-K} \text{Dist}_{pa}$, and is referred to as the *continuity disk*. In other words, if there is no any other knowledge, the best prediction of the parallax of p_i is equal to a within the continuity disk.

The principal problem of propagation is to select the proper well-defined reference point. In the constraint triangle surrounding the point p_i , there are three candidate reference points, such as the vertices a , b , and c . Even though it can be expected that the nearest well-defined reference point has more influence on the definition of candidate match's continuity disk in most cases, yet in our method, only the reference point with the highest matching reliability ψ as will be described will be selected for the match propagation. Once the reference point is determined, the chief task is to propagate the match from the reference point to the candidate match point p_i , i.e., to find its conjugate point from set P' . If there is no conjugate point matched according to the parallax limit defined as Equation 4, the match is considered as a null match. If there are multiple candidate conjugate points for p_i , the one with the highest matching reliability ψ is the result. Thus, the matched corner is called the *best matched point*.

The third step of the propagation procedure is to refine the triangulation by inserting the best matched point into it. The new matched point is therefore used as a new well-defined reference point in the subsequent matching process. In an iterative matching propagation procedure, an increasing number of new matched points will be obtained and inserted to the triangulation until a pre-defined criteria is reached.

Matching Reliability Measurement

Each matched point-pair has two important attributes, the parallax and the reliability. In a stereopair such as that shown in Figure 3, the vertices a , b , and c are points in the left image which form a triangular propagation area. Their conjugate points a' , b' , and c' form a corresponding triangle in the right image. Their corresponding epipolar lines are represented as dotted lines. Let the image space coordinates of point a and a' be (u, v) and (u', v') , then the parallax ρ is the difference of coordinates between the reference point-pair:

$$\rho = a' - a = \begin{bmatrix} u' - u \\ v' - v \end{bmatrix}. \quad (5)$$

The reference point pair (a, a') should satisfy the epipolar constraint and the correlation constraint within a fixed tolerance (Zhong and Zhang, 2002). The reliability ψ defined in Equation 6 is used to quantitatively measure the matching reliability:

$$\psi(r, d, d') = r \times f(\sqrt{d^2 + d'^2}), \quad (6)$$

$$f(x) = \begin{cases} 1 - \frac{x}{\sigma} & \text{if } 0 \leq x \leq \sigma \\ 0 & \text{else} \end{cases} \quad (7)$$

where, σ is a threshold to describe the extent satisfying the epipolar constraint, d and d' are the distances of points a and a' to their corresponding epipolar lines as shown in Figure 3 c, r is the zero-mean normalized cross-correlation

measure for a (m, n) window around the points a and a' respectively, which is invariably between -1 and 1 , and is defined as:

$$r = \frac{\sum_{i=1}^m \sum_{j=1}^n [(x_{ij} - \bar{x})(y_{ij} - \bar{y})]}{\sqrt{\sum_{i=1}^m \sum_{j=1}^n (x_{ij} - \bar{x})^2} \sqrt{\sum_{i=1}^m \sum_{j=1}^n (y_{ij} - \bar{y})^2}} \quad (8)$$

$$\bar{x} = \frac{1}{m \times n} \sum_{i=1}^m \sum_{j=1}^n x_{ij} \quad (9)$$

$$\bar{y} = \frac{1}{m \times n} \sum_{i=1}^m \sum_{j=1}^n y_{ij} \quad (10)$$

where x_{ij} and y_{ij} are gray level values of the pixels in correlation windows.

The matching reliabilities of the other two matched point pairs (b, b') and (c, c') are also calculated in the same manner.

Implementational Issues

Issue One

In each single loop of the recursive matching propagation procedure, a set of image corner points in each triangle area will be extracted at first, and the best one (if there is) is then matched out using the aforementioned method. For corner extraction, there are two different strategies, i.e., performed globally in the whole image, or performed in each triangle separately. If globally extracting all the corners before matching propagation process, the matching process could be quicker, but it is harder to control the completeness of the results because among the candidate corners there would be a lot of null matches. However, if dynamically extracting the corners in each triangle area during the matching propagation procedure, it is convenient to enable the density of matched points adaptive to the terrain characteristics. For example, the matching propagation can be ended in a triangle when there is no proper matched point, or when the size of triangle area is small enough, or when the total matched points number is accepted.

Issue Two

During the matching propagation procedure, it is significant to quickly find the triangle enclosing a point for both the refinement of the triangulation mesh dynamically by inserting new matched points and the selection of the well-defined reference points for a candidate match. A fast and reliable method is the so-called "walk through triangulation" algorithm proposed by Mucke *et al.* (1996). To find a triangle that contains a new point, the algorithm starts from any arbitrary triangle and finds the homogeneous coordinates of the new point with respect to each edge of the triangle. If all the area coordinates of the point are positive, then the point falls within this triangle. If not, we walk across the edge that has negative coordinates and repeat the same procedure for the new triangle. This method is proved to take expected computation time close to $O(n^{\frac{1}{2}})$ for point location in two dimensional Delaunay triangulation of n random points (Su and Drysdale, 1997; Sundareswara and Schrater, 2003).

Issue Three

The refinement of triangulation by inserting a new matched point is not only to split the triangle enclosing the point into three, but also to update all the influenced adjacent

triangles according to the Delaunay criterion. For example, a fast and reliable insertion method is first to eliminate this triangle and any adjacent triangles that contain this new point in their circumcircle, and then to retriangulate the resulting empty spot. The expected time to insert a new point is roughly $O(n)$ where n is the current number of points (Su and Drysdale, 1997).

Experimental Testing

In order to investigate the reliability and accuracy of the matching method described above, a Supresoft's VirtuoZo[®] NT[®] (a commercial DPW made in China) is selected as the reference platform for the photogrammetric processing of real aerial stereopairs. Our choice of the VirtuoZo[®] NT[®] as a reference platform is under the two considerations: the first reason is its accuracy. Baltsavias *et al.* (1996) investigated the digital terrain model (DTM) generation by Leica/Helava's DPW 770 with SOGET SET[®] digital photogrammetric software and VirtuoZo[®] NT[®] digital photogrammetric systems, and concluded that both systems (DPW 770 and VirtuoZo[®] NT[®]) are useful for automatic DTM generation and deliver similar accuracy. Another consideration concerns its availability; VirtuoZo[®] NT[®] is now widely used in the production of digital terrain models and digital orthoimages in China.

In order to test the stability and effectiveness of this new matching method, there are four different aerial stereopairs used in our experiment, which are taken from four types of land-cover, i.e., the flat area and the water area with poor textures, the building area, and the mountainous area with better textures.

TABLE 1. COMPARISON RESULTS BETWEEN THE NEW MATCHING METHOD AND THE EXISTING METHOD

Accuracy Check Points	New Method		Existing Method	
	RMSE ₀ (m)	Max ₀ (m)	RMSE ₁ (m)	Max ₁ (m)
Building area	0.103	0.317	0.268	0.692
Water area	0.337	1.071	0.879	3.331
Mountainous area	0.182	0.464	0.207	0.815
Flat area	0.210	0.439	0.252	0.877

The experiment is straightforward and can be divided roughly into five main parts:

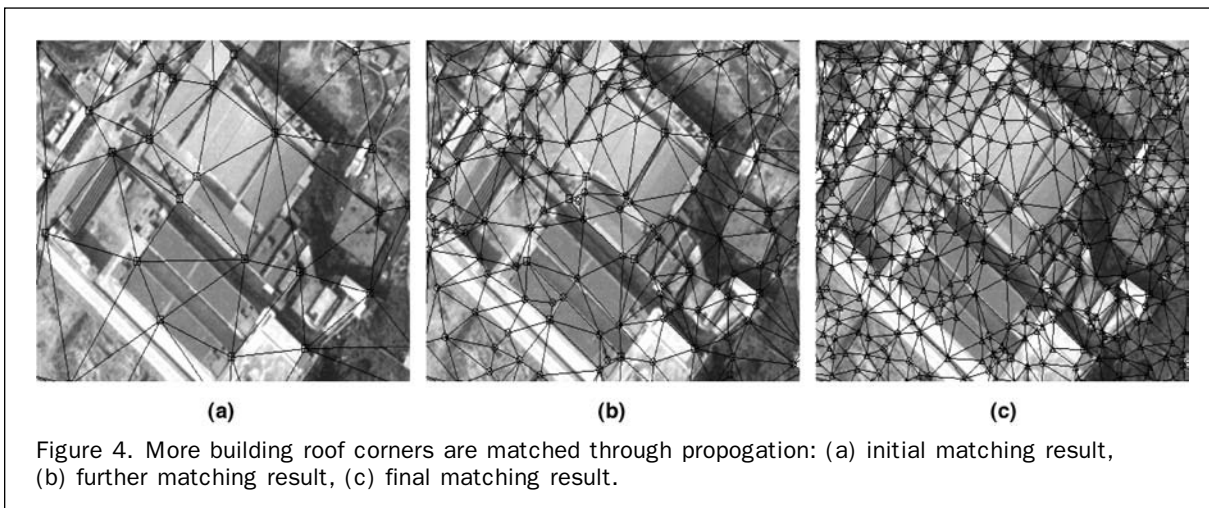
- (1) VirtuoZo[®] NT[®] is used for all the inner orientation and relative orientation, and to generate the four epipolar stereopairs. After these processes, a first set of well-defined point pairs within 181 to 200 points for each stereopair are collected.
- (2) Four gridded digital surface models are automatically generated by VirtuoZo[®] NT[®] (with $492 \times 839 = 412,788$ points).
- (3) Based on the epipolar stereopairs, the adaptive triangle constrained image matching is carried out. The maximum number of matched points is used to end the match propagation. Four triangulated digital surface models with 412,788 points (the same points number as that generated by VirtuoZo[®] NT[®]) were obtained automatically.
- (4) For comparison purposes, 200 checkpoints for each stereopairs were measured manually using VirtuoZo[®] NT[®]. The locations of these checkpoints are distributed over four types of terrain surfaces.
- (5) The manually measured elevations of the checkpoints are compared with the bilinear interpolated values at the corresponding planimetric positions from digital surface models generated by VirtuoZo[®] NT[®] and our new method, respectively.

The comparison results are listed in Table 1, where, RMSE₀ is the root mean square error (RMSE), and max₀ is the maximum error of the checkpoints generated by our method, respectively. RMSE₁ and max₁ are the RMSE and the maximum error of the checkpoints generated by VirtuoZo[®] NT[®].

Conclusions

From the results shown in Table 1 and as illustrated in Figure 4 through Figure 7, the experimental testing conveys the following conclusions:

- (1) Generally speaking, the matching accuracies of the new matching method are higher than the existing method, the RMSEs of checkpoints were decreased by 12 percent to 62 percent, and the largest errors were decreased about two times.
- (2) Most building corners and specific object boundary points can be matched directly and accurately, thus the matching accuracies in both building and water areas are obviously improved, the RMSEs are decreased by 61.6 percent and 61.7 percent, respectively. As shown in Figure 4, this kind of triangulated irregular network models are useful for further automatic three dimensional reconstruction of a building's geometric surface model. Our future work will be based on



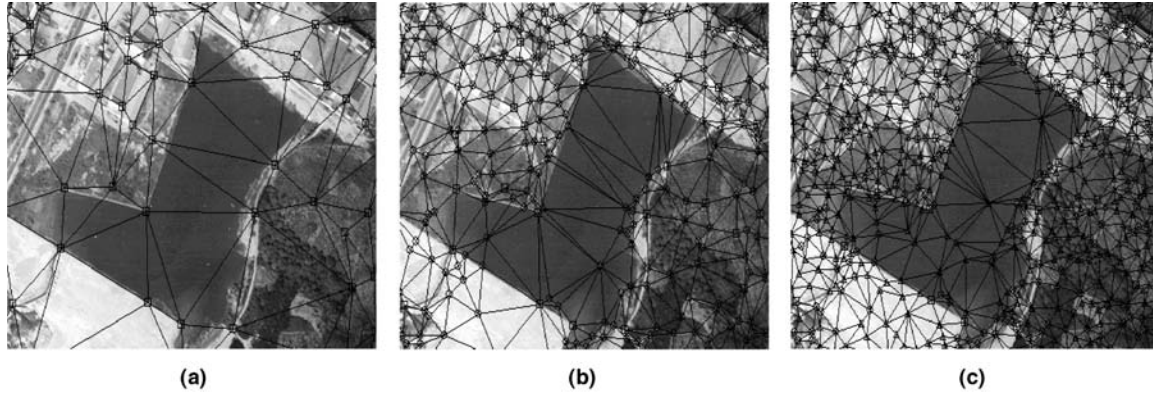


Figure 5. The matching propagation in a water area of poor texture: (a) initial matching result, (b) further matching result, (c) final matching result.

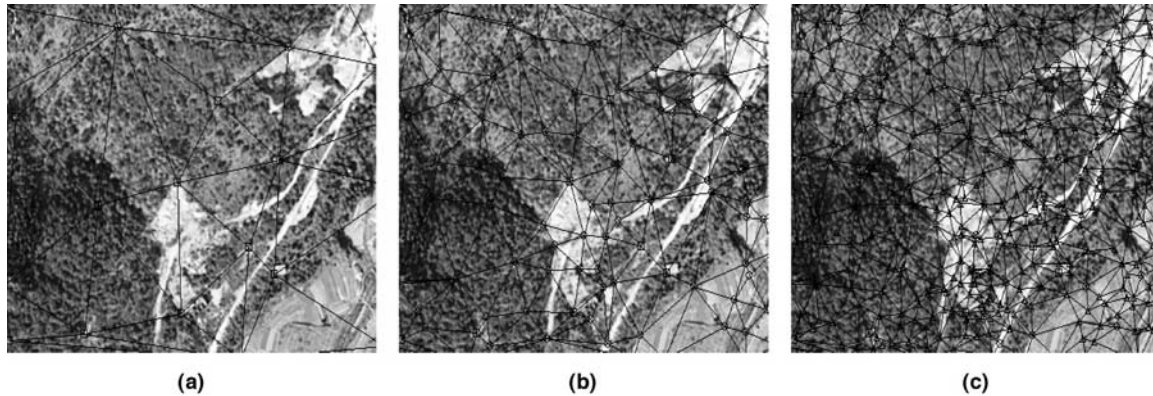


Figure 6. The matching propagation in a mountainous area: (a) initial matching result, (b) further matching result, (c) final matching result.

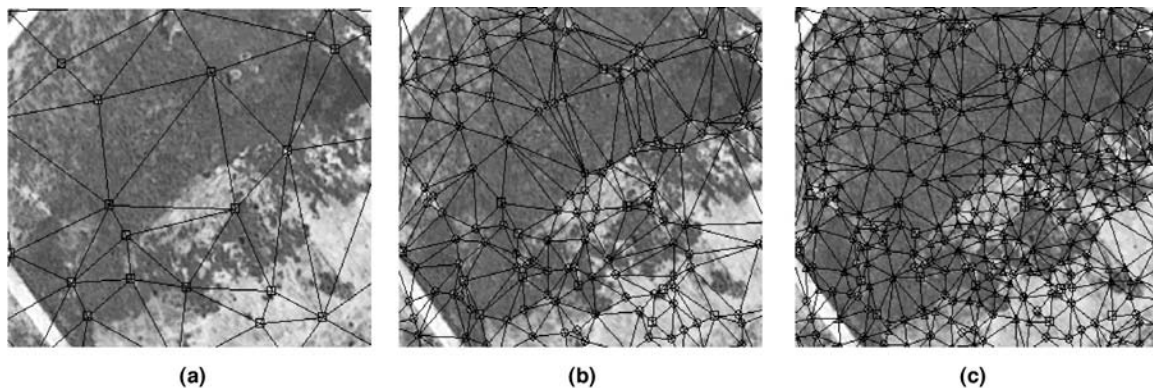


Figure 7. The matching propagation in a flat area: (a) initial matching result, (b) further matching result, (c) final matching result.

such kind of digital surface models to automatically extract and reconstruct the 3D geometry of buildings.

- (3) The false matching caused by occlusion and repetitive texture in texture-poor areas is reduced to a minimum by

using various corners and the local geometric constraint. As shown in Figure 5 and Figure 7, the local continuity constraint is increasingly and explicitly enforced while the triangulation is being refined iteratively in texture-poor

areas such as the water area and the flat area. As listed in Table 1, all the maximum errors of checkpoints from the four different types of terrain areas were decreased greatly. The subsequent interactive edit workload could thus be reduced to the minimum.

- (4) The completeness of the resulting digital surface models is better than those done through traditional methods, and the density of the resulting triangulation models is obviously self-adaptive to the terrain characteristics or the image texture features.

Acknowledgments

The authors are indebted to Professor Zhilin Li (Department of Land Surveying and Geo-Informatics, Hong Kong Polytechnic University) for his critical comments and helpful suggestions during the writing of this paper. All the reviewers' comments and remarks to this paper are appreciated very much. The work described in this paper is supported by (No: 2002CB312101), the Croucher Foundation, the Hong Kong Research Grant (CUHK4132/99H), and the China "863" High-Tech Development Program (2001AA135130).

References

- Baltsavias, E.P., H. Li, S. Gaschen, and M. Sinning, 1996. DTM generation with the Leica/Helava DPW 770 and VirtuoZo digital photogrammetric systems, *Proceedings of the Symposium Geoinformatics'96*, Wuhan, China, pp. 10–17.
- Bern, M., and D. Eppstein, 1992. Mesh generation and optimal triangulation, *Computing in Euclidean Geometry, Lecture Notes Series on Computing* (D.Z. Du and F. Hwang, editors), World Scientific, Singapore, Vol.1, pp. 23–90.
- Boufama, B., and K. Jin, 2002. Towards a fast and reliable dense matching method, *Proceedings of Vision Interface 2002*, Calgary, Canada, pp. 178–185.
- Heipke, C., 1993. Performance and state-of-the-art of digital stereo processing *Photogrammetric Week'93*, pp. 173–183.
- Heipke, C., 1996. Overview of image matching techniques, *Proceedings of OEEPE Workshop on the Application of Digital Photogrammetric Workstations*, Lausanne, Switzerland, Part III.
- Heipke, C., 1997. Automation of interior, relative, and absolute orientation, *ISPRS Journal of Photogrammetry and Remote Sensing*, 52:1–19.
- Heipke, C., 2001. Digital photogrammetric workstations – a review of the state-of-the-art for topographic applications, *GIM International*, 15(4):35–37.
- Lawson, C.L., 1977. Software for C1 surface interpolation, *Mathematical Software III* (J.R. Rice, editor), Academic Press, New York, pp. 161–194.
- Lhuillier, M., and L. Quan, 2000. Robust dense matching using local and global geometric constraints, *Proceedings of the 16th International Conference on Pattern Recognition*, Barcelona, Spain, Vol. 1, pp. 968–972.
- Mucke, E.P., I. Saias, and B. Zhu, 1996. Fast randomized point location without preprocessing in Two- and Three-dimensional Delaunay Triangulations, *Proceedings of the 12th Annual Symposium on Computational Geometry*, pp. 321–330.
- Pollard, S., J. Porrill, J. Mayhew, and J. Frisby, 1986. Parallax gradient, lipschitz continuity, and computing binocular correspondence, *Robotics Research: The Third International Symposium*, (O.D. Faugeras and G. Giralt, editors), MIT Press, pp. 19–26.
- Sundareswara, R., and P.R. Schrater, 2003. Extensible Point Location Algorithm, *International Conference on Geometric Modeling and Graphics (GMAG'03)*, London, pp. 84–89.
- Schmid, C., R. Mohr, and C. Bauckhage, 2000. Evaluation of interest point detectors, *International Journal of Computer Vision*, 37(2):151–172.
- Su, P., and R. Drysdale, 1997. A comparison of sequential Delaunay triangulation algorithms, *Computational Geometry: Theory and Applications*, (7):361–386.
- Tang, L., H.T. Tsui, and C.K. Wu, 2002. Dense stereo matching based on propagation with a voronoi diagram, *Proceedings of India Conference on Computer Vision, Graphics and Image Processing III*, Ahmedabad, India, pp. 230–240.
- Tuceryan, M., and T. Chorzempa, 1991. Relative sensitivity of a family of closest point graphs in computer vision applications, *Pattern Recognition*, 25:361–373.
- Zhang, Z., and Y. Shan, 2000. A progressive scheme for stereo matching, *ECCV Workshop SMILE2*, Dublin, pp. 1796–1803.
- Zhong, Y., and H.F. Zhang, 2002. Control Points based semi-dense matching, *Proceedings of the 5th Asian Conference on Computer Vision*, Melbourne, Australia, pp. 137–144.

(Received 25 February 2004; accepted 20 May 2004; revised 01 June 2004)